Comparison of Precipitate Behaviors in Ultra-Low Carbon, Titanium-Stabilized Interstitial Free Steel Sheets under Different Annealing Processes

J. Shi and X. Wang

(Submitted 3 January 1999; in revised form 29 July 1999)

Ultra-low carbon, titanium-stabilized interstitial free (ULC Ti-IF) steel sheets are widely used in the automobile industry because of excellent deep drawability. The annealing process is critical to their final property, and there are two different annealing processes used in industrial production of interstitial free (IF) steel sheets, namely batch annealing and continuous annealing. In this study, precipitation behaviors of titanium IF steels in the two annealing processes were investigated. Among the most common precipitates in titanium IF steels, that is, TiN, TiS, $Ti_4(CS)_2$, and TiC, the size and dispersion of TiN, TiS, and $Ti_4(CS)_2$ remained almost unchanged after either annealing process. Conversely, the average size of a TiC particle increased substantially after both annealing processes, while TiC after continuous annealing was larger than that after batch annealing due to the higher heating temperature of continuous annealing. Two new particles, FeTiP and (Ti, Mn)S, were also observed in the batch annealing process but not in continuous annealing. The structure of FeTiP and (Ti, Mn)S were studied, and furthermore the evolution of FeTiP precipitation was found to be closely related to recrystallization in batch annealing. Finally, the interrelation among processing parameters, precipitation behaviors, and final property was studied.

Keywords batch annealing, behaviors, continuous annealing, interstitial free steel, precipitate, recrystallization

1. Introduction

Interstitial free (IF) steels are referred to as the steels from which the remaining carbon and nitrogen atoms in solution are scavenged as the precipitates by the addition of titanium and/or niobium to achieve high deep drawability and the nonaging property for the steel sheets. For commercial ultra-low carbon, titanium-stabilized interstitial free (ULC Ti-IF) steels, the scavenging effect of titanium renders not only the ferrite matrix almost interstitial free but also gives rise to the formation of precipitates such as TiN, $Ti_4(CS)_2$, TiS, and TiC. The precipitation behavior during industrial production processes, like reheating and hot rolling, influences the final properties of IF steels.

For ULC Ti-IF steel sheets, precipitation mainly occurs in the processes of steelmaking, slab reheating, hot rolling, and coiling. The different processing parameters, such as temperature, time, and/or reduction ratio of these processes have their effects on the size, shape, and distribution of precipitates, and in turn influence deep drawability. For example, low slab reheating temperature can cause a sparse distribution of coarse precipitates, and then the pinning effect of particles during annealing is substantially reduced, thus yielding strong {111} texture and high deep drawability (Ref 1). In recent years, there have also been many research papers dealing with the precipitation behavior of TiC, TiS, and $Ti_4(CS)_2$ during hot rolling (Ref 2), the quantitative analysis of precipitates of titanium IF steels (Ref 3), thermodynamic calculation of maximum solute carbon and nitrogen concentrations (Ref 4), and so on. However, those investigations were mainly concerned with the precipitation before cold rolling. As for the precipitation behavior during annealing, there are a very limited number of papers. For example, Satoh (Ref 5) studied the carbide dissolution in continuous annealing and the interaction with dislocation in annealing. Furthermore, studies dealing with batch annealing and its effect on recrystallization have not yet been conducted as far as the authors know.

J. Shi, School of Industrial Engineering, Purdue University, West Lafayette, IN 47907; and **X. Wang,** School of Materials Science and Engineering, University of Science and Technology Beijing, China. Contact e-mail: jshi@ecn.purdue.edu.

2. Experimental Procedures

Two types of cold-rolled titanium-IF steel sheets obtained in mass industrial production were used as the experimental materials for the annealing simulation in the lab. Steelmaking was completed in the plant of a steel company with further treatment in vacuum degassing facilities and casted on continuous slab casters. Hot rolling was performed on a continuous wide strip mill, and cold rolling was carried out on a five stand mill. The same hot-rolling and cold-rolling reduction rates were used for the two materials. Table 1 lists the chemical composition and processing parameters. The IF1 is a typical titanium IF steel with normal chemical composition, and the main research work of this study was on IF1. In comparison to IF1, material IF2 has a similar composition and nearly identical processing parameters except for coiling temperature. The purpose of this study was to investigate the influence of coiling temperature on precipitate behavior.

Batch annealing and continuous annealing simulation were carried out in the lab. It should be noted here that the simulation

parameters were determined based on actual industrial annealing processing records. For continuous annealing simulation, the cold-rolled samples were heated to 850 °C in a salt bath furnace at a rate of 10 °C/s with a soaking time of 150 s, and then cooled in the air. For the batch annealing simulation, nitrogen was used as protecting gas in a heat treating furnace. The samples were first heated to 350 °C at 80 °C/h, and then were heated to 710 °C at 50 °C/h with a soaking time of 4 h, and finally cooled with the furnace. For research on interaction between recrystallization behavior and precipitation, samples were quenched from various temperatures during heating in the continuous annealing and batch annealing simulation processes.

The extracted carbon replica specimens for transmission electron microscope (TEM) were observed with a JEM-200CX. The average diameter and size distribution of particles were analyzed and calculated by an image analyzer. Most precipitates in extracted replicas were identified by energy dispersive x-ray spectrometry (EDS), and the criterion for distinguishing TiS and $Ti_4(CS)_2$ was based on the relative ratio of two peak heights of titanium and sulfur. Meanwhile, the phase structures of some precipitates were calculated from electron diffraction patterns and EDS. Optical microscopy was used to study the microstructural change in samples. The texture was measured by x-ray diffraction on a Rigaku 2038 (Rigaku International Corp., Tokyo, Japan), and the orientation distribution function (ODF) was computed from the three incomplete pole figures {110}, {200}, and {112}.

3. Results and Discussion

3.1 Observation of TiS, TiN, and $Ti_4(CS)_2$

Table 2 summarizes the different stages of processing, namely, hot rolling, cold rolling, and batch annealing/continuous annealing, for the size of TiN, TiS, and $Ti_4(CS)_2$. It is obvious that the average sizes of those precipitates nearly remained unchanged, and the distributions of TiN, TiS, and $Ti_4(CS)_2$ were random in all the four stages. However, the quantity of TiS and/or $Ti_4(CS)_2$ in batch annealed samples was apparently less

Table 1 Chemical composition and processing parameters of materials

Materials	Composition, %						Reheating temperature, °C	Finish rolling temperature, °C	Coiling temperature, °C
	C	N	S	Ti	Mn	P			
IF1	0.0035	0.0028	0.0041	0.076	0.17	0.01	1227	892	690
IF2	0.0045	0.0030	0.0040	0.069	0.15	0.01	1246	892	635

Table 2 Size of TiN, TiS, and $Ti_4(CS)_2$ in IF1 during different stages of processing

Precipitates	Diameter range of precipitates, nm			
	Hot rolled	Cold rolled	After batch annealing	After continuous annealing
TiN	200-1100	176-1000	180-1400	200-1200
TiS	40-420	50-350	40-500	40-450
$Ti_4(CS)_2$	100-500	80-550	80-600	100-540

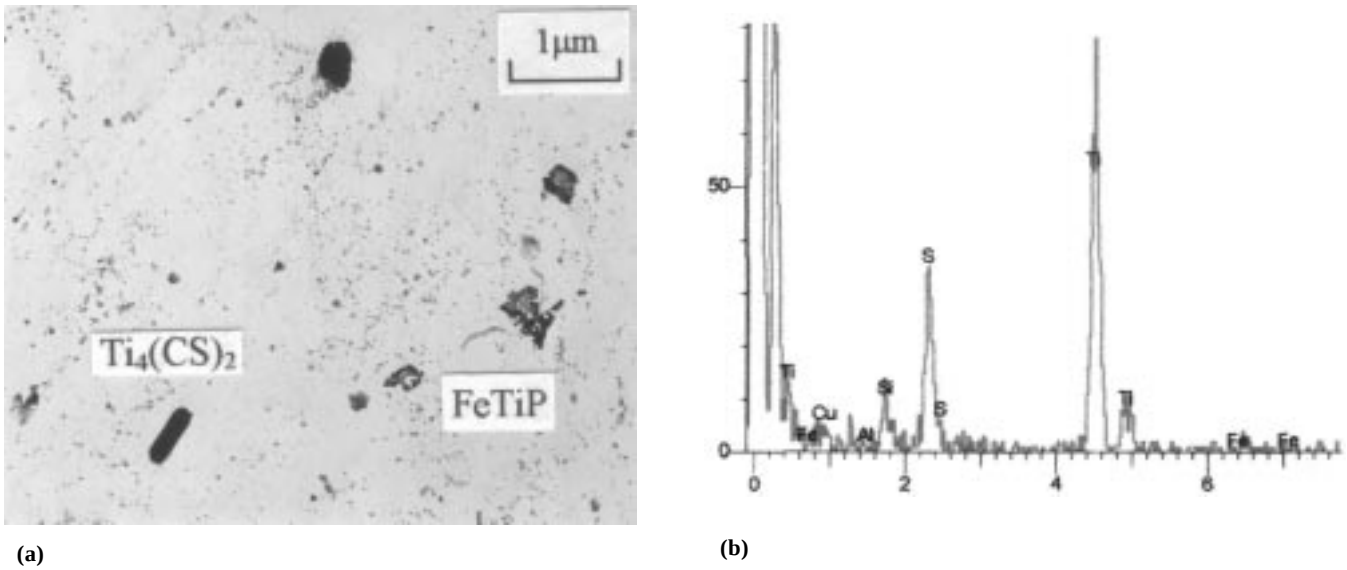

(a) **(b)**

Fig. 1 A rectangular-shaped $Ti_4(CS)_2$ remaining in batch annealed IF1. (a) Transmission electron microscopy. (b) Electron dispersive x-ray spectra

than that in hot-rolled and continuous annealed samples, which stands for the dissolution of TiS under low annealing temperature of 710 °C with long soaking time. In addition, it was observed that some large particles such as TiN and TiS precipitates were broken in cold rolling, and some regular-shaped particles precipitated in the slab reheating phase still remained in full annealed samples. Figure 1 shows a rectangular-shaped $Ti_4(CS)_2$ particle existing in full batch annealed IF1.

3.2 Comparison of TiC Evolution in Batch Annealing and Continuous Annealing

The TiC is also a common type of precipitate in titanium IF steels, but it is finer and has a denser distribution than TiN, TiS, and $Ti_4(CS)_2$. In contrast to TiN, TiS, and $Ti_4(CS)_2$ in annealing, TiC particles change both in size and in dispersion. For the two materials used in this experiment, fine TiC particles, which distribute in hot band densely and randomly, coarsened and distributed sparsely after annealing. In addition, it is easy to observe TiC particles distributed on the grain boundaries in continuous annealed samples, while this rarely occurs in batch annealed samples, as shown in Fig. 2. It can be inferred that batch annealing leads to longer recovery period for cold-deformed grain, which helps grain boundaries bypass fine TiC under low grain growth speed; while short soaking time and high activation energy of continuous annealing makes TiC particles move with grain boundaries during rapid recrystallization.

Figure 3 shows the quantitative analysis result of the TiC size in steel IF1 under four different processing stages. From this figure, it can be seen that the average diameters of TiC particles in hot-band and in cold-rolled IF steels do not change much, and the average diameters of TiC particles in annealed samples are larger than that of TiC in hot-band and cold-rolled samples. The TiC in the continuous annealed sample has the largest average diameter, which is about 23.5 nm, and its single maximum diameter exceeds 60 nm. From the previously given results, it is not difficult to understand that annealing temperature plays an important role in affecting the size of TiC particles, and soaking time is far less important. The annealing temperature of continuous annealing is normally above 830 °C, which is higher than the TiC dissolution temperature for ULC Ti-IF steels. So, in spite of the short soaking time of continuous annealing, TiC particles are easier to dissolve, reprecipitate, and coarsen. Furthermore, it is believed that TiC moving with grain boundaries in rapid recrystallization of continuous annealing also gives rise to the coarsening effect. In this way, TiC in a continuous annealing sample exhibits the largest average diameter.

3.3 Precipitation of New Particles in Annealing

Aside from the difference in the morphology of TiN, TiS, $Ti_4(CS)_2$, and TiC between the batch annealed and continuous annealed IF steels, the main difference is that FeTiP and (Ti, Mn)S precipitate in batch annealing, but not in continuous annealing. In this aspect, it appears that the long heat history of batch annealing is helpful to the precipitation of new particles, while the very short heat history of continuous annealing is not. The FeTiP has been found in IF steels containing high phosphorus and high manganese (Ref 7), but rarely found in commercial ULC Ti-IF steels. Also, for high phosphorus, high strength IF steels, FeTiP precipitation has been reported in the coiling process with coiling temperature higher than 700 °C (Ref 8). However, FeTiP was not observed in hot bands of the two materials, even after coiling temperatures from 630 to as high as 760 °C were used in hot-rolling simulation in the lab. Meanwhile, it has been reported that TiS exists with the encapsulation of MnS in hot-band or annealed IF steels (Ref 7, 9). In the study, it should be noted that individual MnS particles were never found in all four stages for both Ti-IF steels, and (Ti, Mn)S only precipitated in batch annealing.

Through EDS quantitative analysis for dozens of (Ti, Mn)S particles, it was found that titanium, manganese, and sulfa have a nearly fixed atom ratio of 45 to 10 to 45. From this, (Ti, Mn)S could not possibly be a mixture of TiS and MnS. Instead, it should be a single and uniform phase. Because the diameters of

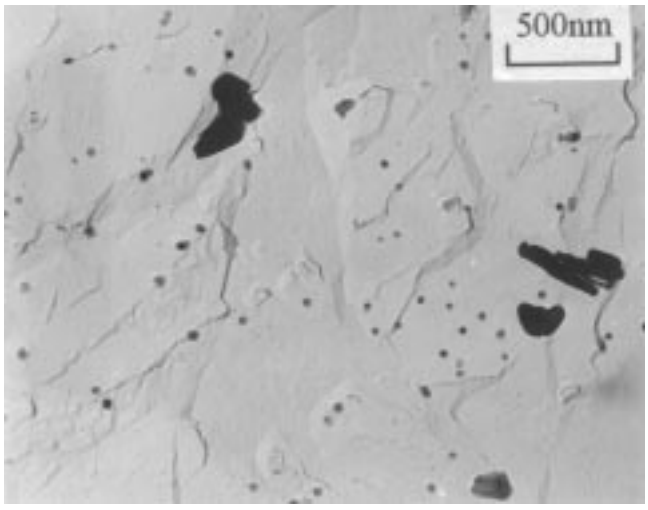

(a)

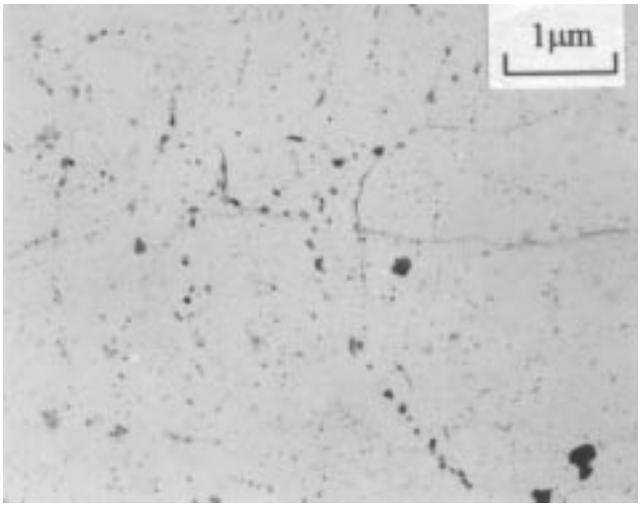

(b)

Fig. 2 Transmission electron micrograph of typical dispersion of TiC particles in (a) batch annealed IF1 and (b) continuously annealed IF1

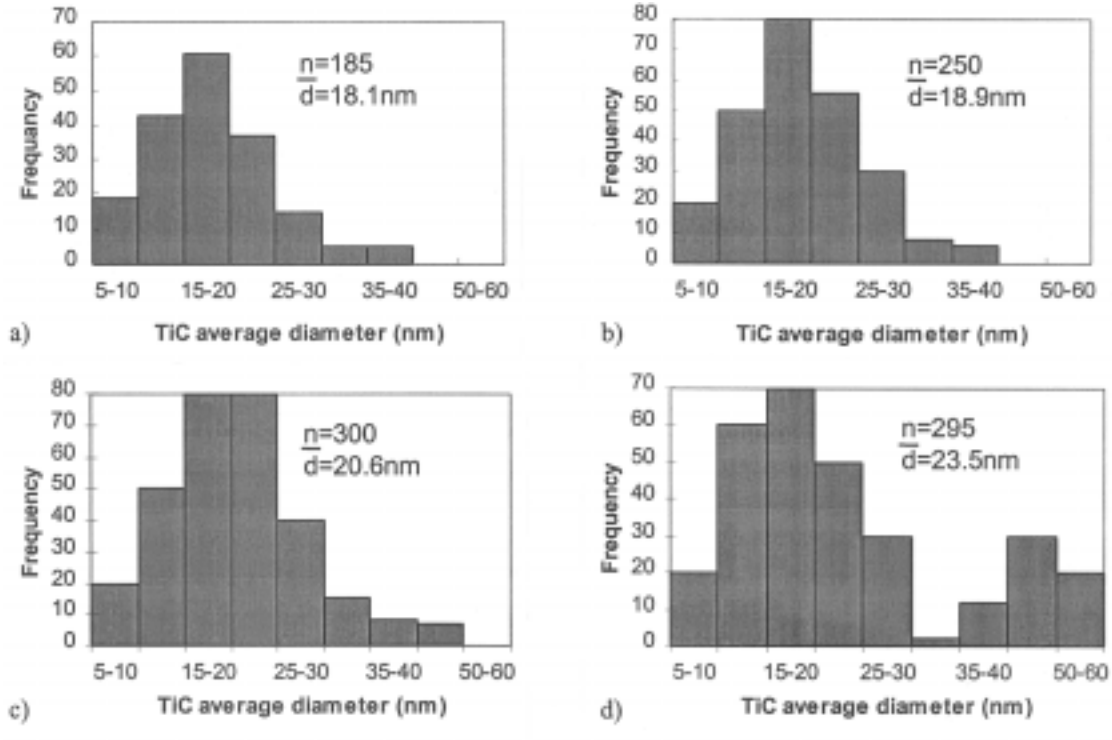

Fig. 3 The TiC precipitate size distribution in IF1 under different stages of processing. (a) Hot rolled. (b) Cold rolled. (c) Batch annealed. (d) Continuously annealed

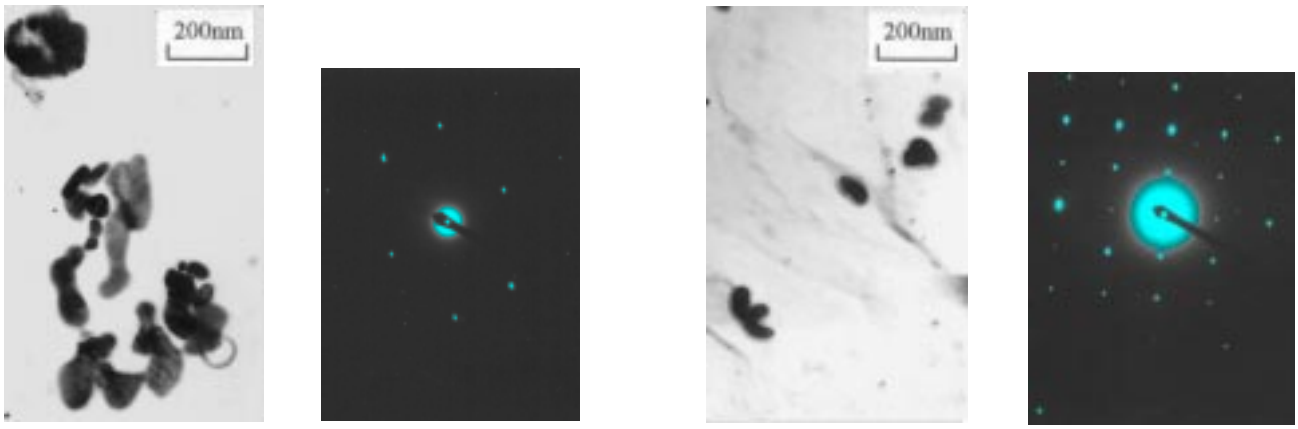

Fig. 4 Transmission electron micrograph and electron diffraction pattern of typical FeTiP morphology in batch annealed (a) IF1 and (b) IF2

titanium and manganese are close, (Ti, Mn)S was suggested to be the result of manganese atoms replacing part of titanium atoms in TiS, which makes the phase structure of (Ti, Mn)S similar to that of TiS. Similarly, FeTiP is also a single phase, and its atom ratio of iron, titanium, and phosphorus is about 34 to 33 to 33. When electron diffraction patterns of FeTiP are measured, calculated, and combined with the corresponding EDS spectra, it is clear that FeTiP owns a hexagonal structure. As far as research has demonstrated until now, the lattice constant a_0 of FeTiP is 6.79 Å. After the results were compared with that of many iron-phosphorus compounds in ASTM cards, the FeTiP phase structure was found to be nearly identical to that of Fe_2P (hexagonal structure, a_0 = 5.87 Å and c_0 = 3.46 Å). The difference in lattice constant can be explained by lattice distortion from the atom diameter difference of titanium and iron. So the FeTiP structure is the result of titanium atoms replacing nearly half of the iron atoms in Fe_2P.

Figure 6 illustrates the FeTiP morphology of IF1 samples, which are heated at the same speed of batch annealing simulation and quenched at temperatures of 640, 680, 710, and 750 °C. The FeTiP starts to precipitate at 640 °C when the recovery is almost complete, and primary recrystallization is about to start. As the annealing temperature rises to 680 °C, the amount of FeTiP increases and FeTiP coarsens. When the temperature

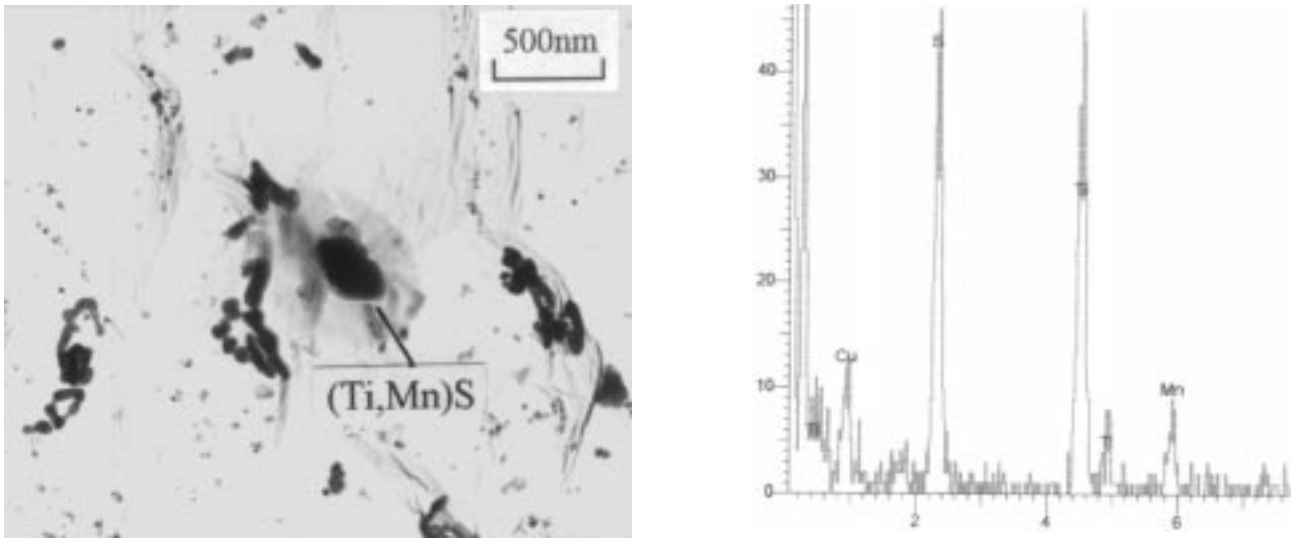

(a) **(b)**

Fig. 5 Transmission electron micrograph and electron dispersive x-ray spectrometry spectra of (Ti, Mn)S in batch annealed IF1

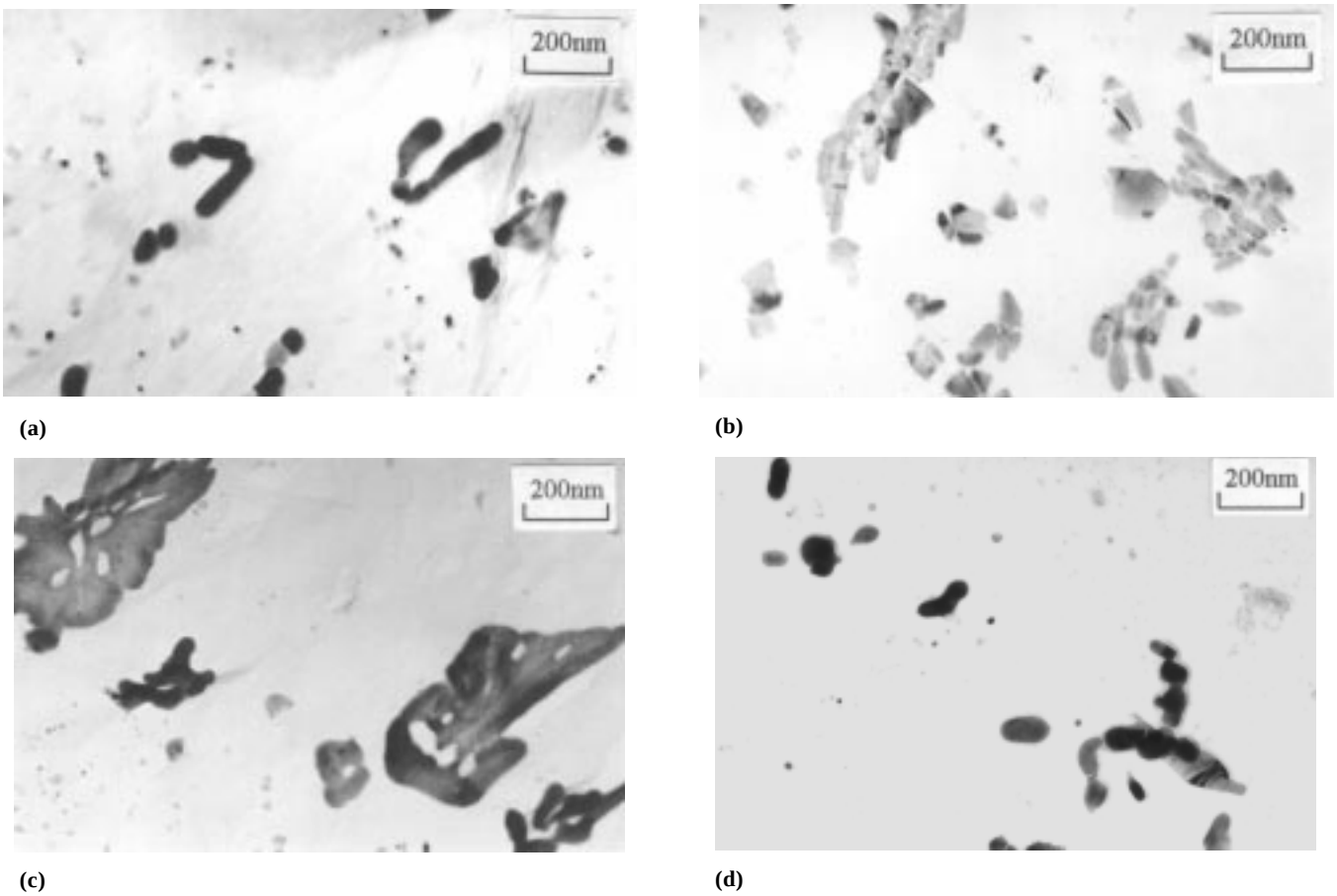

(a) **(b)**

(c) **(d)**

Fig. 6 Transmission electron micrograph of the morphology of FeTiP in IF1 heated at a rate of 50 °C/h, quenched at (a) 640 °C, (b) 680 °C, (c) 710 °C, and (d) 750 °C

reaches 710 °C, the density and size of FeTiP particles continue to rise and reach their peak point in this experiment. But the quantity, size, and density of FeTiP particles decreased when the sample was continuously heated to 750 °C. This means that FeTiP starts to dissolve at that temperature. The precipitation and growth of (Ti, Mn)S particles are somehow like that of FeTiP particles, but they are relatively difficult to observe because they are much less.

As cited previously, FeTiP has been found to precipitate as low as 700 °C with high manganese content. The fact that FeTiP precipitates at 640 °C, which corresponds to the stage of recovery, shows FeTiP precipitation is not only associated with chemical composition and processing temperature, but also soaking time. That is to say, the entire heating history plays a role in FeTiP and (Ti, Mn)S precipitation in batch annealing.

However, interesting research points deserving further investigation still remain, such as the effect of cold rolling on FeTiP and (Ti, Mn)S precipitation, the thermodynamics of FeTiP precipitation, the interaction between dislocation and these precipitates, and so on.

3.4 Influence of New Precipitates in Batch Annealing on Texture Development

The chemical composition and processing parameters of IF1 and IF2 are very close, and their cold-rolling and batch annealing simulation processes are identical. In addition, the hot bands of the two materials exhibit similar grain size. The only difference is that the coiling temperature of IF1 (690 °C) is higher than that of IF2 (635 °C) by 55 °C. According to the common knowledge about IF steels, high coiling temperature is helpful to obtain high $\bar{r}$ value, so IF1 should exhibit higher $\bar{r}$ value than IF2. But in fact the γ-fiber texture of IF2 is stronger than that of IF1, as shown in Fig. 7, and the $\bar{r}$ value of IF2 is higher than that of IF1 by 0.2.

It is thought that the difference in precipitation may play an important role in the variation of texture intensity and $\bar{r}$ value. As far as it is concerned, it should be divided into the effect of the precipitates formed before annealing and the effect of the precipitates formed during annealing.

In the case of titanium and/or niobium added IF steels, a number of particles formed before annealing have been found to have extremely different effects on cold-rolling texture and annealing texture according to different publications. For example, it has been suggested that the precipitates, NbC and Ti(C, N), in IF steels are largely irrelevant with respect to the formation of {111} annealing texture (Ref 6). On the contrary, other works (Ref 1, 10) have shown that the particles have strong pinning effect on the grain boundary mobility during recrystallization growth, and the effect is believed to be an important factor for controlling the annealing texture in IF steels. According to the author's study (Ref 11), TiC and the other precipitates before cold rolling do not have any substantial effect on recrystallization and texture evolution.

Actually, for the batch annealed steels IF1 and IF2, no obvious difference in the morphology of TiS, TiN, and $Ti_4(CS)_2$ has been observed. Both TiC distributions are mainly within the grains. In addition, it has been observed that the average TiC size in IF1 is slightly larger than that in steel IF2 by about 3 nm, which is believed to be due to coiling temperature effect. So, in terms of TiC, steel IF2 has more mole faction, which is due to its high carbon content, and has less average diameter. According to the commonly accepted pinning model (Ref 12-14) the supposed pinning effect of TiC in IF2 should be more severe, and the delay of recrystallization should be more significant. However, it contradicts the actual result. Thus, the effect of precipitates before annealing is not the main reason.

The precipitate formed during annealing is another potential factor. Generally speaking, if the precipitation occurs before or during recrystallization, there will be interaction (Ref 6). There was much more FeTiP precipitating in IF1 through transmission electron microscopy observation. Figure 8 shows the typical FeTiP morphology of the two batch annealed steels. The size and quantity of FeTiP are larger in steel IF1 than in steel IF2. It is well known that solute phosphorus exists in IF ferrite matrix as a substitution atom, and it tends to segregate on grain boundary (Ref 15). If the FeTiP particles precipitate, many of them will disperse along grain boundaries, have a strong pinning effect on the movement of new grain, and then hinder grain growth and the formation of recrystallization texture. Figure 9 shows how FeTiP locates on grain boundaries in 80% recrystallized IF1, which strongly hinders grain growth and γ-fiber texture development. In this way, the precipitation of FeTiP retards recrystallization. The precipitation of FeTiP in IF1 is much more than that in IF2, and its pin effect is much stronger; hence a relatively less intense γ-fiber texture develops in IF1 and with lower $\bar{r}$ value.

Although no FeTiP particles precipitate in the coiling process despite a very high coiling temperature, according to this study, coiling temperature does indirectly affect FeTiP precipitation during batch annealing. The higher the coiling temperature, the more the FeTiP precipitation in batch annealing.

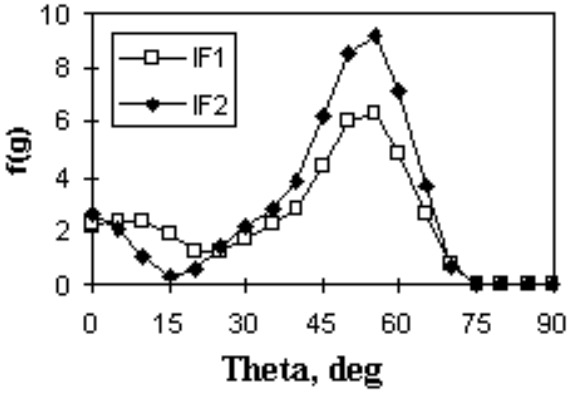

(a)

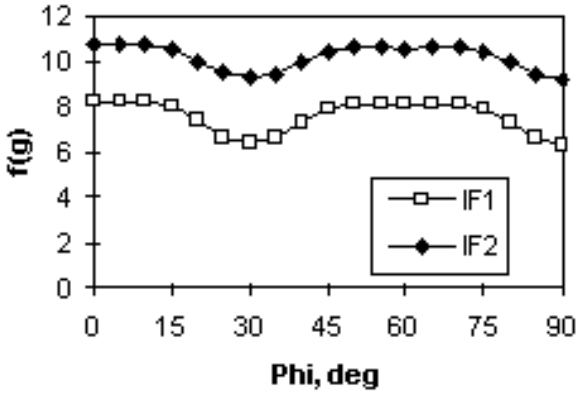

(b)

Fig. 7 Comparison of α-fiber and γ-fiber textures of batch annealed IF1 and IF2. (a) α-line. (b) γ-line

Therefore, as far as FeTiP precipitation is concerned, high coiling temperature is not always helpful for obtaining good deep drawability for IF steels through batch annealing.

4. Industrial Implication

It is well recognized that improper chemical composition ratio and processing parameters will cause poor deep drawability for ULC Ti-IF steels. In many steel companies, the effort to obtain optimum alloy content or processing parameters has never stopped. However, the difference between batch annealing and continuous annealing has not been well studied and considered in determining the chemical composition and processing parameters. This study shows the necessity of selecting different hot-rolling parameters for IF steels if the following annealing processes are not identical.

In a project aimed at increasing the qualification rate of IF steel production in a steel company, where over 80% of IF steels are produced through batch annealing, the authors have analyzed the production data of thousands of coils. It was found that about 70% of the unqualified coils were due to poor composition or processing problems, but the rest, 30%, could meet the requirement of composition and processing parameters. The previously discussed IF1 steel sheet is one of the cases: its $\bar{r}$ value should be above 2.0, but actually it was 1.9. After enough attention was given to the important effect of precipitation behavior in batch annealing, the puzzle was then solved.

For many steel companies, batch annealing was widely used for producing commercial ULC IF steels. The suggestions from this study are the following: (a) Phosphorus content is also an important index in alloy design of ULC IF steels, and it should be as low as possible. (b) Low coiling temperature (<680 °C) is recommended if phosphorus content is high. (c) High heating rate is preferred in order to avoid unfavorable precipitation in annealing. In a word, it is really a new challenge to improve the deep drawability of batch annealed IF steels through precipitate control.

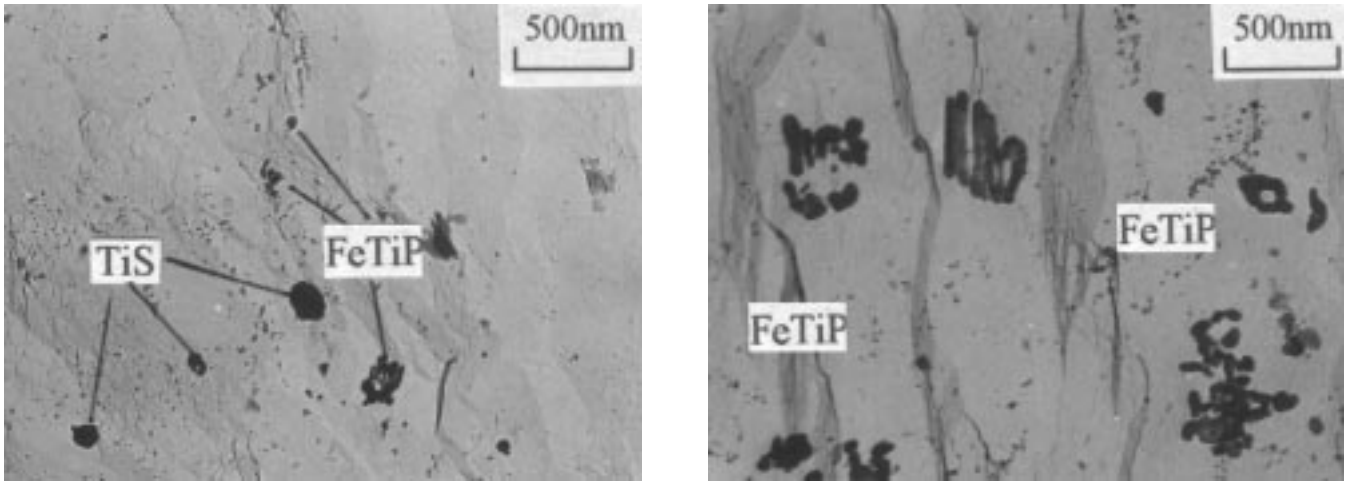

(a) **(b)**

Fig. 8 Comparison of FeTiP morphology between batch annealed IF1 and IF2

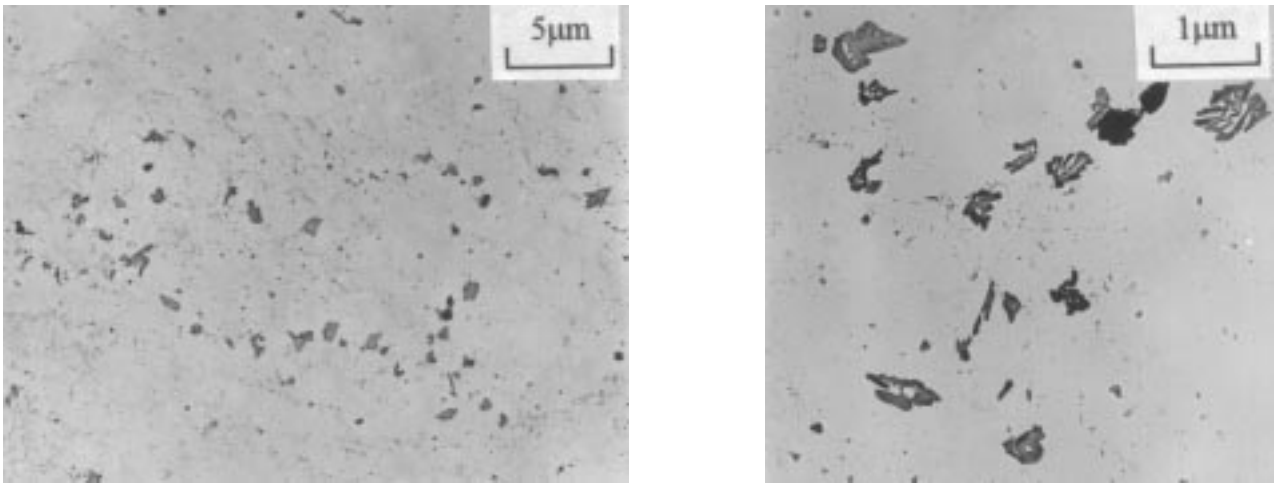

(a) **(b)**

Fig. 9 Dispersion of FeTiP along grain boundaries in batch annealed IF1

5. Conclusions

The following conclusions can be drawn:

- There is no significant change in average diameter, morphology of TiN, TiS, and $Ti_4(CS)_2$ between hot-band, cold-rolled, and batch annealed/continuously annealed samples.
- The TiC coarsens and concentrates obviously after both batch annealing and continuous annealing. Because annealing temperature plays a more important role than soaking time in terms of TiC evolution, the average diameter of TiC after continuous annealing was larger than that after batch annealing. In addition, some TiC particles in continuous annealed IF steels apparently distribute on grain boundaries, while the TiC in batch annealed samples distribute more randomly.
- For the commercial ULC Ti-IF steels with low phosphorus (≤0.01%) and low manganese (<0.2%), FeTiP and (Ti, Mn)S precipitate during batch annealing, but they do not precipitate in continuous annealing. This is the main difference of precipitate behavior of Ti-IF steels between batch annealing and continuous annealing.
- The atom ratios of titanium, manganese, and sulfur are around 45 to 10 to 45 for (Ti, Mn)S, and the atom ratios of iron, titanium, and phosphorus are 34 to 33 to 33 for FeTiP. The FeTiP has the hexagonal structure close to that of Fe_2P. Under simulation conditions, FeTiP and (Ti, Mn)S precipitate just before recovery ends. The quantity and size of FeTiP increases to a peak value at about 710 °C, and FeTiP starts to dissolve before 750 °C.
- Although FeTiP and (Ti, Mn)S do not precipitate during coiling even with high coiling temperature, FeTiP precipitation in batch annealing is indirectly affected by coiling temperature, that is to say, the amount of FeTiP increases as coiling temperature increases. The FeTiP precipitation in batch annealing hinders the recrystallization process, and it is harmful for obtaining strong annealing texture and high $\bar{r}$ value. The more the FeTiP is, the weaker the γ-fiber texture and the worse the deep drawability.

Acknowledgments

The authors are grateful for the financial support from the National Key Research and Development Project of the Peoples Republic of China under contract 95-527-01-01-09. The authors acknowledge with gratitude the TEM sample preparation and observation work from Mr. Cong Wang, supply of materials from Baoshan Iron & Steel Corporation located in Shanghai, China, and numerous valuable discussions about industrial production of IF steel with Senior Engineer Binyu Kong and other experts from China's steel industry.

References

1. S.V. Subramanian and J. Gao, Effect of Precipitate Size and Dispersion on Lankford Values of Titanium Stabilized Interstitial-Free Steels, *Proceedings International Forum for Physical Metallurgy of IF Steels* (Tokyo, Japan), Iron and Steel Institute of Japan, 10-11 May 1994, p 53-56
2. G. Tither, C.I. Garcia, M. Hua, and A.J. DeArdo, Precipitation Behavior and Solute Effects in Interstitial-Free Steels, *Proceedings International Forum for Physical Metallurgy of IF Steels* (Tokyo, Japan), Iron and Steel Institute of Japan, 10-11 May 1994, p 293-322
3. A. Belyansky, V. Kapnin, and Y. Larin, Dispersed Particles in IF-Steels and Their Transformation in the Production Process, *Proceedings International Forum for Physical Metallurgy of IF Steels* (Tokyo, Japan), Iron and Steel Institute of Japan, 10-11 May 1994, p 289-292
4. S. Akamatsu, M. Hasebe, T. Senuma, Y. Matsumura, and O. Akisue, Thermodynamic Calculation of Solute Carbon and Nitrogen in Nb and Ti Added Extra-Low Carbon Steels, *ISIJ Int.*, Vol 34 (No. 1), 1994, p 9-16
5. S. Satoh, M. Morita, and O. Hashimoto, Carbide Dissolution in Interstitial Free Steels during Continuous Annealing, *Proceedings Developments in the Annealing of Sheet Steels*, The Minerals, Metals & Materials Society, 1992, p 177-188
6. R.K. Ray, J.J. Jonas, and R.E. Hook, Cold Rolling and Annealing Textures in Low Carbon and Extra Low Carbon Steels, *Int. Mater. Rev.*, Vol 39 (No. 4), 1994
7. A. Okamoto and N. Mizui, Texture Formation in Ultra-Low-Carbon Titanium Added Cold-Rolled Sheet Steels Containing Manganese and Phosphorus, *Proceedings Metallurgy of Vacuum-Degassed Steel Products* (Indianapolis, IN), The Minerals, Metals & Materials Society, 1990, p 161-180
8. K. Ushioda, N. Yoshinaga, and O. Akisue, Influences of Manganese on Recrystallization Behavior and Annealing Texture Formation of Ultra-Low-Carbon and Low-Carbon Steels, *ISIJ Int.*, Vol 34 (No. 1), 1995, p 85-91
9. Z. Wang, "Effect of Metallurgical Factors on the Properties of High Strength IF Steels," Ph.D. thesis, University of Science and Technology Beijing, 1994 (in Chinese)
10. S. Satoh, T. Obara, and K. Tsunoyama, Effect of Precipitate Dispersion on the Recrystallization Texture of Niobium-Added Extra-Low Carbon Cold-Rolled Steel Sheet, *Trans. Iron Steel Inst. Jpn.*, Vol 26 (No. 8), 1986, p 737-744
11. J. Shi, "Study on the Optimization of Batch Annealing Process and Recrystallization Texture Evolution for IF Steels," Ph.D. thesis, University of Science and Technology Beijing, Jan 1998 (in Chinese)
12. P. Hellman and M. Hillert, Effect of Second-Phase Particles on Grain Growth, *Scand. J. Metall.*, Vol 4 (No. 5), 1975, p 211-219
13. M. Hillert, Zener's Pinning Effect—Role of Dispersed Particles on Grain Size Control, *Proceedings THERMEC '88* (Tokyo, Japan), Vol 1, The Iron and Steel Institute of Japan, 6-10 June 1988, p 30-38
14. N. Louat, The Resistance to Normal Grain Growth From a Dispersion of Spherical Particles, *Acta Metall.*, Vol 30 (No. 7), 1982, p 1291-1294
15. K. Matsudo, T. Shimomura, K. Osawa, M. Sakoh, and S. Ono, Effect of Phosphorus on the Deep Drawability of Cold Rolled Steel Sheets, *Proceedings 6th International Conference on Texture of Materials* (Tokyo, Japan), Vol 2, Iron and Steel Institute of Japan, 1982, p 759